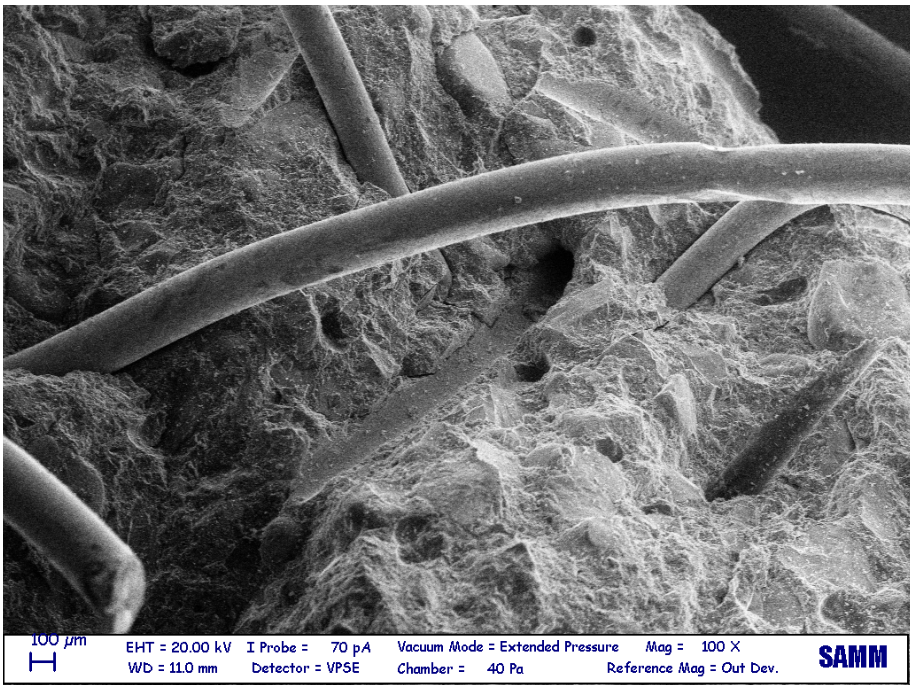

COVER PICTURE
SEM image of a fracture surface of a specimen of UHPFRC.
Immagine al microscopio elettronico a scansione di una superficie di frattura di un campione di UHPFRC.

CARATTERIZZAZIONE DI DUE CALCESTRUZZI UHPFRC COMMERCIALI
Valutazione di proprietà meccaniche e di durabilità

Bianca Paola Maffezzoli
Politecnico di Milano, Dipartimento di Chimica, Materiali e Ingegneria Chimica "Giulio Natta"
biancapaola.maffezzoli@polimi.it

Dario Redaelli
HES-SO, University of Applied Sciences Western Switzerland, Freiburg, Switzerland
dario.redaelli@hefr.ch

Elena Redaelli
Politecnico di Milano, Dipartimento di Chimica, Materiali e Ingegneria Chimica "Giulio Natta"
elena.redaelli@polimi.it

SOMMARIO

Questa nota presenta i risultati di una ricerca volta a valutare e confrontare le proprietà di due calcestruzzi fibrorinforzati ad altissime prestazioni (UHPRFC) commerciali realizzati con la stessa quantità di fibre di acciaio (2.5% vol.). Oltre ad una caratterizzazione di base delle proprietà meccaniche, come la resistenza alla compressione e il modulo elastico, sono stati misurati alcuni parametri correlati alla durabilità, quali la resistività elettrica, la resistenza alla carbonatazione e alla penetrazione dei cloruri, la velocità di assorbimento e l'assorbimento d'acqua. Inoltre, è stata osservata la microstruttura mediante microscopia ottica ed elettronica. I risultati hanno mostrato che, sebbene le fibre possano localmente aumentare la porosità della pasta cementizia all'interfaccia e ridurre la resistività elettrica, entrambi i calcestruzzi hanno mostrato un comportamento complessivamente eccellente, in particolare se confrontati con i calcestruzzi ordinari.

ABSTRACT
CHARACTERIZATION OF TWO COMMERCIAL UHPFRC MIXTURES
Assessment of mechanical and durability parameters

This note presents the results of a research aimed at assessing and comparing the properties of two commercial Ultra-High-Performance Fiber Reinforced Concretes (UHPRFC) made with the same amount of steel fibers (2.5% vol.). Besides the basic properties at hardened state, such as compressive strength and elastic modulus, durability-related parameters are measured, such as electrical resistivity, resistance to carbonation and chloride penetration, water absorption rate and water absorption. Microstructure is also studied by means of optical and electron microscopy. The results show that, although fibers may locally increase the presence of interfacial voids in the cement paste and decrease the electrical resistivity of UHPFRC, both products exhibited an overall excellent behavior if compared to ordinary concrete.

PAROLE CHIAVE | KEYWORDS
Calcestruzzo, UHPFRC, durabilità
Concrete, UHPFRC, durability

INTRODUCTION

Ultra-High-Performance Fiber Reinforced Concrete (UHPFRC) is characterized by a very low water/binder ratio (about 0.2), the addition of supplementary cementitious materials such as silica fume or ground granulated blast furnace slag and the lack of coarse aggregate, which result in a very compact microstructure and a low porosity. Moreover, UHPFRC is reinforced with fibers (mostly steel fibers) which provide crack opening control, which is an important aspect for practical applications [1]. These characteristics provide an excellent mechanical behavior, with compressive strength higher than 120 MPa and a strain-hardening behavior in tension. UHPFRC is therefore considered as a material with an intrinsically excellent behavior in terms of durability as well. As such, besides applications for structures exposed to aggressive environments, it is often used for the repair and retrofitting of existing structures that are damaged by deterioration phenomena, such as corrosion [2,3].

The composition of UHPFRC can be designed to achieve tailored properties: for instance, at fresh state, either self-compacting or thixotropic behavior can be obtained by using different superplasticizers; at hardened state, a self-healing behavior is often achieved thanks to the high dosages of binder, specifically cement [4]. Although some "home-made" recipes are used for experimental research [5,6], practical applications still resort to commercial products that come in the form of dry powders containing pre-mixed binders and aggregates of unknown type and proportions.

This study presents the results of an experimental research aimed at characterizing two commercial UHPFRCs, named UHPFRC-D and UHPFRC-V. UHPFRC-D is supplied in the form of a dry powder (that includes binders and aggregates), steel fibers and a superplasticizer. UHPFRC-V is supplied as a dry powder which only includes binders, while the remaining ingredients (aggregates, fibers and superplasticizers) can be chosen by the user and are mixed together with water in proportions given by the producer.

Compressive strength and elastic modulus are measured to assess the mechanical behavior; capillary suction, water absorption, ultra-sonic pulse velocity and electrical resistivity, carbonation and chloride diffusion tests are carried out together with microstructural analysis to characterize the durability of these UHPFRCs. Both mechanical and durability properties are measured on specimens that have been wet cured for different durations.

MATERIALS AND METHODS

The selected UHPFRCs are prepared with the same fibers content (2.5% in volume). The materials used for UHPFRC-D are a commercial dry premix (premix D, including all the solid components, i.e., cement, silica fume and fine aggregate of unknown nature), high-strength steel fibers (straight, brass-coated, 14 mm long and 0.2 mm in diameter) and a polycarboxylate ether (PCE) superplasticizer. The producers declare a water-cement ratio below 0.21 with the provided recipe. To cast UHPFRC-V, a commercial premix (premix V, including just the binder components, i.e., cement and slag in unknown proportion) is mixed together with quartz powder (maximum diameter 0.25 mm), steel fibers of the same type as those used in UHPFRC-D and a PCE superplasticizer. For this mixture, the producers declare a water-cement ratio of 0.2. Table 1 summarizes the materials used and their recipes, with dosages in kg/m^3 provided by the producers.

Table 1. UHPFRC materials and recipes.

Component	UHPFRC-D	UHPFRC-V
Premix D (kg/m^3)	2146	-
Premix V (kg/m^3)	-	980
Water (kg/m^3)	134	196
Quartz powder 0-0.25 mm (kg/m^3)	-	1150
PCE superplasticizer (kg/m^3)	36	22
Steel fibers (% in volume)	2.5	2.5
Steel fibers (kg/m^3)	187	187
w/c	< 0.21	< 0.22

The mixing procedure is essentially the same for the two products and it is summarized in table 2. Dry powders are mixed first, then water and superplasticizer are added and, after reaching a homogeneous mix with the desired workability, fibers are added. Both mixtures had a slump flow of 890-925 mm and fulfilled the target properties at fresh state declared by the producers.

Table 2. UHPFRC mixing procedures.

UHPFRC-D	UHPFRC-V	Time
Add premix and mix	Add premix and mix	2 min
	Add aggregates and mix	3 min
Add water and superplasticizer and mix until the desired workability is reached	Add water and superplasticizer and mix until the desired workability is reached	10 min
Add fibers and mix	Add fibers and mix	3 min
Casting	Casting	

Cylindrical specimens of diameter 70 mm and height 140 mm (obtained by casting in cylindrical molds) are used for mechanical characterization and mass per unit volume measure, while cylinders of diameter 100 mm and height 50 mm (obtained by coring and cutting specimens cast in cubic molds of 100 mm) are used for all other tests.
Mechanical characterization is performed by measuring compressive strength and elastic modulus, after measuring the mass of the cylindrical specimens.
Ultrasonic pulse velocity test is carried out on dried 7 and 28 wet cured specimens by applying two probes on opposite surfaces and measuring the velocity of ultrasounds inside concrete.
Capillary suction tests are carried out on specimens dried in oven at 40°C up to constant mass. The absorbed water mass is measured over time and the correlation between the water absorbed per unit surface and the square root of time is calculated. The initial linear correlation is interpolated with the least squares method to obtain the so-called initial absorption rate or sorptivity (S), which is generally correlated with concrete porosity and pore size distribution.
Water absorption indicates the maximum amount of water that UHPFRC can absorb (i.e., in the saturation condition), which allows to estimate the total porosity. Water absorption tests are carried out on specimens which are initially dried in oven at 100°C up to constant mass and then submerged in water at T = 20°C up to constant mass. Water content is calculated over time as the mass of absorbed water divided by the dry mass of the specimen in percentage.

The electrical resistivity is an important parameter for concrete durability since it is correlated to the corrosion condition of the steel rebar embedded in concrete after depassivation (lower electrical resistivity corresponds to higher corrosion risk [7]) and it is calculated through the conductance which is measured directly through two copper plates placed on opposite surfaces of the specimens. The electrical resistivity depends on porosity and water content inside concrete and therefore it is measured concurrently with the water content during immersion up to saturation condition.
A natural diffusion test is performed to measure UHPFRC resistance to chlorides penetration, which is an essential aspect since most applications imply exposure to aggressive environments [8]. Specimens are submerged in a solution with 3.5% of NaCl for approximately 9 months. At the end of this exposure, the specimens are ground with depth steps of approximately 1 mm and the resulting powder is digested in nitric acid and analyzed with potentiometric titration to obtain the chlorides content at different depths. In this way, the chlorides penetration profile is obtained. The interpolation of the chloride's penetration profile with Fick's law (1) provides the values of chlorides diffusion coefficient and of chlorides concentration at the surface.

$$C/C_s = 1-\mathrm{erf}(x/2\sqrt{(D_{app} \cdot t)}) \quad (1)$$

In equation 1, C is the chlorides concentration at depth x, C_s is the chlorides concentration at the surface, x is the depth, D_{app} is the chlorides diffusion coefficient and t is the exposure time.
Carbonation resistance is measured by exposing specimens in a chamber with 3% of carbon dioxide (at T = 20°C and RH = 65%) for 4 months. The carbonation penetration depth is revealed by spraying a phenolphthalein solution on a freshly cut surface of the specimens. This indicator reveals change in pH and becomes pink where concrete is still alkaline.
As far as microstructural analyses are concerned, the "thin section technique" is used. A thin section consists of a 25 μm thick slice of UHPFRC impregnated with a fluorescent epoxy and glued on a slide. For each UHPFRC, a thin section is obtained. Due to this impregnation, all air-filled spaces in the concrete (e. g., air-voids, capillary pores, and cracks) are filled with fluorescent dye and are visible as light green zones when viewed in the fluorescent light mode of an optical microscope. In addition, one fragment of each UHPFRC is observed with the stereomicroscope and with the scanning electron microscope (SEM).
All the tests are carried out in duplicate except chlorides diffusion test, carbonation, and microstructural analyses, which are performed on single specimens. Compressive strength and elastic modulus are measured after 7, 21 and 28 days of wet curing; capillary suction, water absorption, ultra-sonic pulse velocity and electrical resistivity are measured on specimens that are wet cured for 7 and 28 days. Carbonation and chloride diffusion tests are carried out on specimens that are wet cured for 7 days, as well as microstructural analysis by means of optical and electron microscopy. Wet curing of specimens takes place in a climate chamber with T = 20°C and RH = 90%.

RESULTS AND DISCUSSION

Concrete mass per unit volume at hardened state and ultra-sonic pulse velocity at 7 and 28 curing days are reported in table 3. The mass per unit volume at 7 curing days is 2500 kg/m^3 for UHPFRC-D and 2400 kg/m^3 for UHPFRC-V. The ultra-sonic pulse velocity instead is 3549 m/s and 3688 m/s for UHPFRC-D and UHPFRC-V, respectively. At 28 curing days, the values of both parameters are quite similar to those at 7 days. These results indicate an overall good quality of these materials.

Table 3. Mass per unit volume and ultrasonic pulse velocity at 7 and 28 curing days (average between duplicate specimens).

	Curing days	UHPFRC-D	UHPFRC-V
Mass per unit volume (kg/m^3)	7	2500	2400
	28	2490	2410
Ultrasonic Pulse Velocity (m/s)	7	3549	3688
	28	3594	3762

Figures 1 and 2 show the evolution of compressive strength and elastic modulus in time. Average values of compressive strength are quite similar: around 135 MPa and 130 MPa at 28 curing days for UHPFRC-D and UHPFRC-V, respectively. Elastic moduli at 28 curing days are approximatively 55 GPa for UHPFRC-D and 45 GPa for UHPFRC-V.

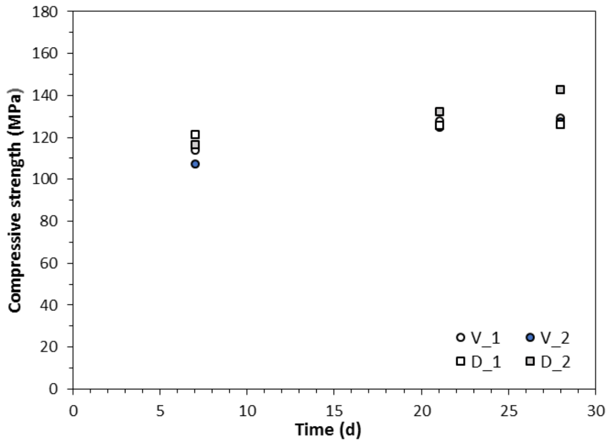

1. Compressive strength of UHPFRC during wet curing.

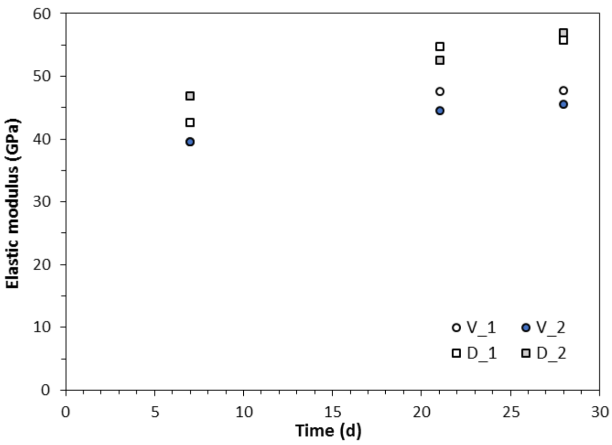

2. Elastic modulus of UHPFRC during wet curing.

Figures 3 and 4 show the amount of absorbed water per unit surface during capillary suction test on specimens wet cured for 7 and 28 days, respectively. UHPFRC-V absorbs more water with respect to UHPFRC-D for both curing times. The initial absorption rate (calculated as the average of the two values from duplicate specimens) at 7 curing days is 0.11 $kg/m^2h^{0.5}$ for UHPFRC-D and 0.27 $kg/m^2h^{0.5}$ for UHPFRC-V. Therefore, UHPFRC-V absorbs water faster than UHPFRC-D, suggesting a higher porosity in UHPFRC-V. However, both values are lower compared to ordinary concrete, where typical values of S are of the order of 0.5 $kg/m^2h^{0.5}$ [9]. The effect of curing (which brings to pore refining due to hydration of cement) is visible in both UHPFRCs, since at 28 days S decreases to 0.08 $kg/m^2h^{0.5}$ for UHPFRC-D and to 0.2 $kg/m^2h^{0.5}$ for UHPFRC-V.

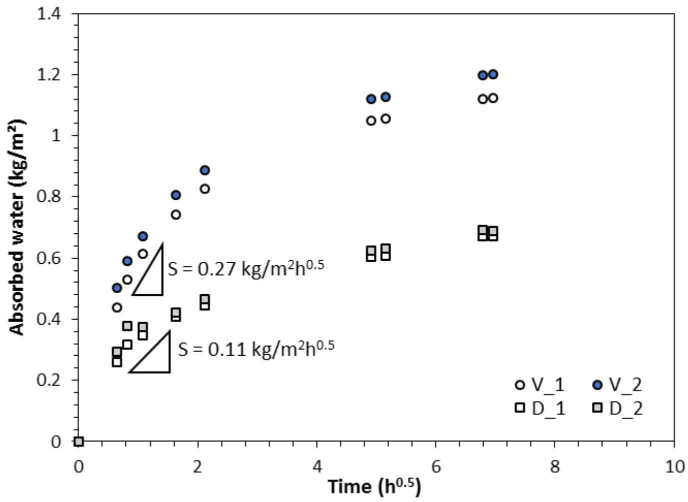

3. Absorbed water during capillary suction test on specimens wet cured for 7 days. Parameter S is the initial absorption rate calculated as the average of the two slopes of the initial linear part of the curves of duplicate specimens.

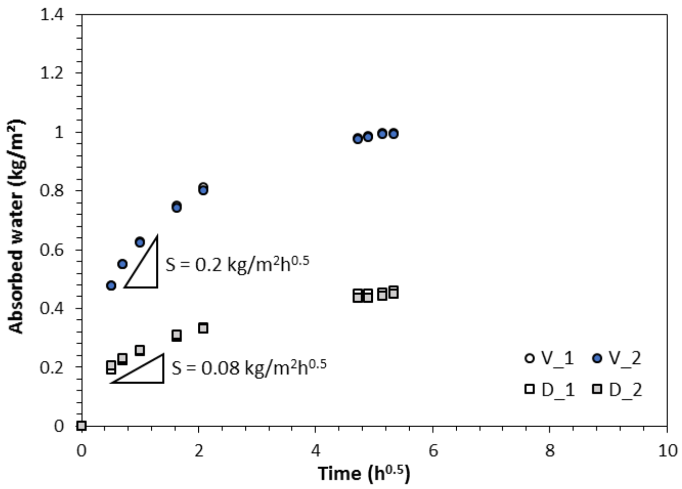

4. Absorbed water during capillary suction test on specimens wet cured for 28 days. Parameter S is the initial absorption rate calculated as the average of the two slopes of the initial linear part of the curves of duplicate specimens.

Figure 5 shows the water absorption values at 7 and 28 curing days. At 7 curing days the absorption is around 1.1% and 1.8% for UHPFRC-D and UHPFRC-V, respectively. At 28 curing days the absorption value is around 0.4% and around 1.1% for UHPFRC-D and UHPFRC-V, respectively. The higher values for UHPFRC-V confirm the higher open porosity of this concrete, however even for this parameter the values are still considerably lower than in ordinary concrete [10], meaning that UHPFRC has a very low open porosity. Also in this case, the effect of pore refining during curing is visible in both UHPFRCs.

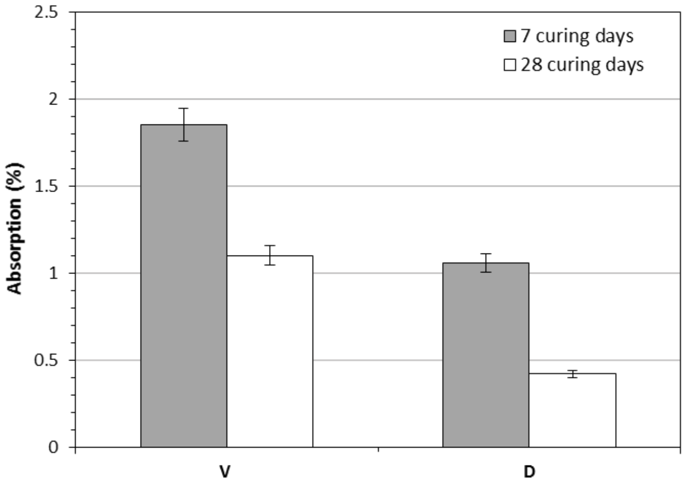

5. Absorption of water at 7 and 28 curing days. Values are calculated as the average between two values measured on duplicate specimens and are reported with errors bars.

Figure 6 shows the electrical resistivity of concrete in saturation condition. At 7 curing days the resistivity is around 500 ohm·m for UHPFRC-D and around 140 ohm·m for UHPFRC-V. At 28 curing days the resistivity is quite similar to the one measured at 7 curing days, with a slight decrease for both concretes: the curing effect is barely visible on this parameter. The lower values for UHPFRC-V confirm the higher open porosity of this concrete since the resistivity is measured in saturation condition and therefore the value is not affected by water content. In this case, the values in saturation condition are similar to those of ordinary concrete [10] even if other parameters obtained on UHPFRC are indicative of a lower porosity. This could be explained by the presence of steel fibers which give a contribution to electrical conduction, resulting in a lower resistivity.

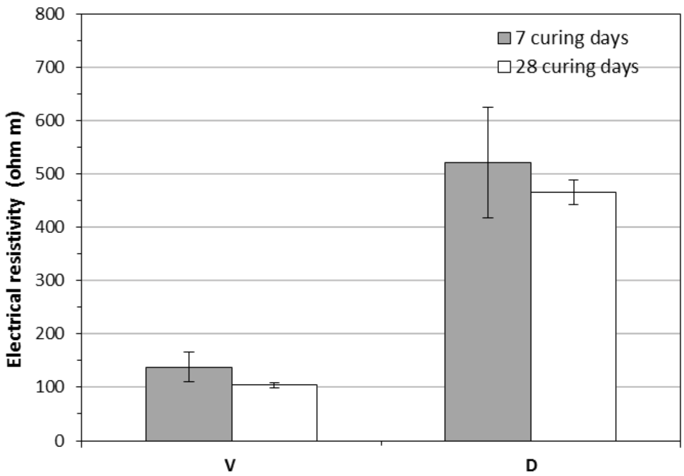

6. Electrical resistivity at 7 and 28 curing days in saturation condition. The values are calculated as the average between two values measured on duplicate specimens and reported with errors bars.

Figures 7 and 8 show the correlation between electrical resistivity and water content of concrete at 7 and 28 curing days, respectively. These measurements were carried out during immersion and the specimens, that were initially dry, progressively absorbed water and increased their water content. Resistivities measured on 28 days wet cured specimens are slightly higher than resistivities measured at 7 curing days, as expected. A growing trend is visible for both concretes and for both curing times: as water is absorbed, the unhydrated cement starts to hydrate and the resistivity increases. This is the same phenomenon that occurs in ordinary concretes during curing, while in UHPFRC it can occur also during service life due to the cement excess [11]. In UHPFRC-D this phenomenon is more evident than in UHPFRC-V, suggesting that the former has a higher amount of unhydrated cement and therefore the effect of a prolongated curing time should affect more positively the durability parameters correlated to porosity. This is confirmed by the results of water absorption and capillary suction tests. Moreover, UHPFRC-D has a higher resistivity compared to UHPFRC-V for specimens with the same humidity content. This fact underlines that the cement paste affects the resistivity of concrete. Despite this phenomenon, the resistivity values are still comparable to resistivities of ordinary concretes. Therefore, more attention should be paid in phenomena in which resistivity is involved, such as corrosion propagation and galvanic coupling between fibers and traditional reinforcing rebar (since UHPFRC is frequently used in combination with steel reinforcement bars).

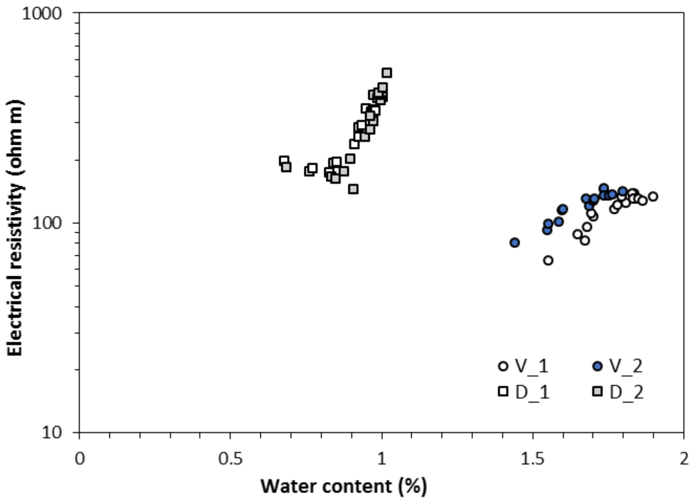

7. Resistivity as a function of water content during immersion at 7 curing days.

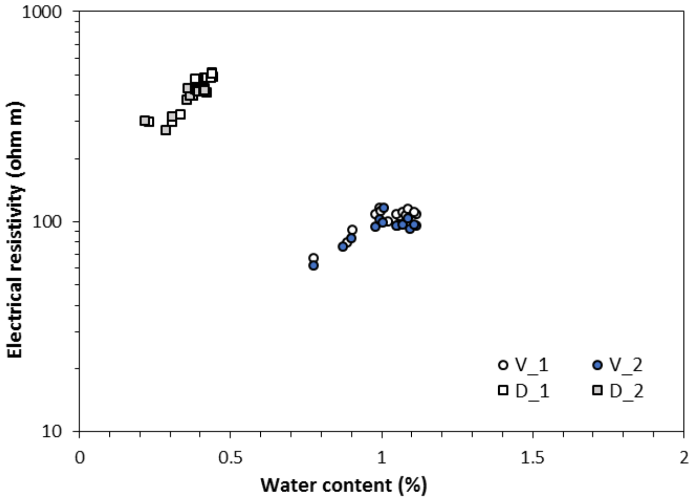

8. Resistivity as a function of water content during immersion at 28 curing days.

Figure 9 shows the chlorides penetration profiles after approximately 9 months of exposure in 3.5% NaCl solution for specimens with 7 curing days (the diffusion tests for specimens cured 28 days are still ongoing). From the penetration profile it is possible to observe that chlorides content becomes nil for depths higher than 4 mm. Moreover, the chlorides concentration at the surface C_s is 1.04% and 1.81% vs. concrete and the diffusion coefficient D_{app} is 0.08 10^{-12} m^2/s and 0.05 10^{-12} m^2/s for UHPFRC-D and UHPFRC-V, respectively. UHPFRC-V has a higher surface concentration and a lower diffusion coefficient compared to UHPFRC-D, this means that the former has a better resistance to chloride penetration even if it has a higher porosity. This may be due to the fact that the natural diffusion of chlorides into concrete is affected not only by porosity but also by other factors, like concrete composition, that can determine the binding ability of concrete towards chlorides.
As far as carbonation is concerned, the carbonation depth is still not detectable after 4 months of exposure to accelerated conditions. The high carbonation resistance could be explained again with the cement excess in the concrete, which provides an "alkalinity reserve" and maintains the pH high. Longer exposure time are required to evaluate carbonation resistance; however, it is unlikely that carbonation can represent a risk for these types of concrete.

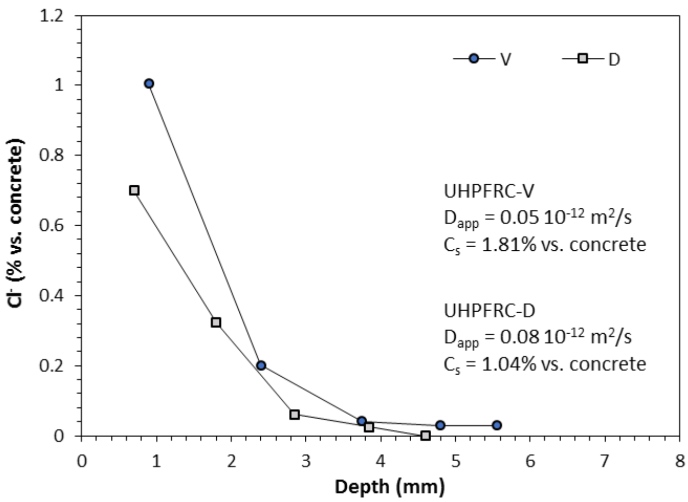

9. Chlorides penetration profile at 7 curing days. D_{app} and C_s are respectively the chlorides diffusion coefficient and the chlorides concentration at the surface deriving from the interpolation of the curve with Fick's law (eq. 1).

Figures 10 and 11 show pictures of thin sections of UHPFRC-D and UHPFRC-V, respectively, taken with the optical microscope in fluorescent light mode. The fluorescent dye shows zones with increased porosity (light green areas in the pictures). Thin section D (figure 10) presents a very compact microstructure with few light green zones, mostly located near the fiber. Thin section V present more areas with increased porosity over all the cement paste. This is consistent with results that indicate a higher porosity of UHPFRC-V with respect to UHPFRC-D. Moreover, a zone with increased porosity is present near a fiber also in concrete UHPFRC-V, suggesting that fibers may locally increase the presence of interfacial voids.

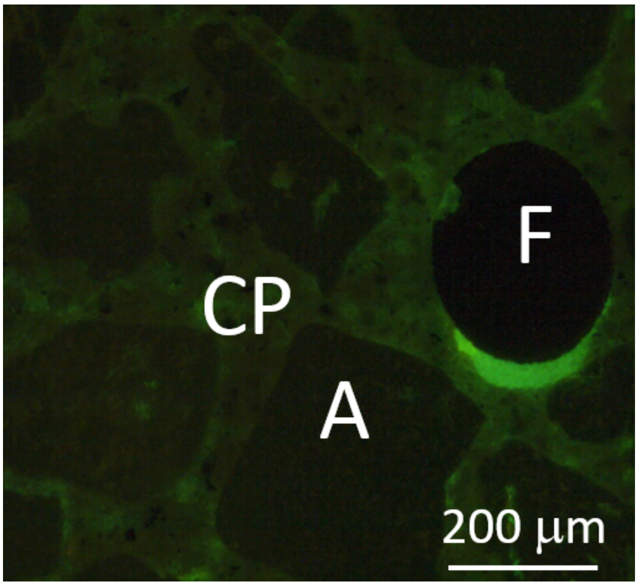

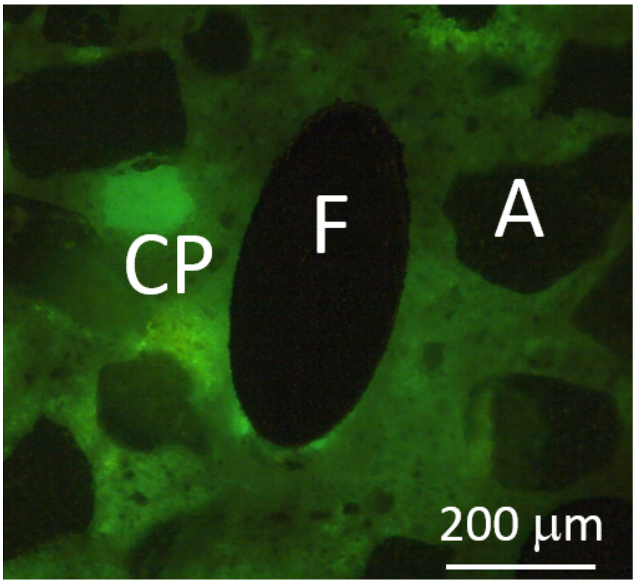

10. Picture of D thin section taken with the optical microscope (fluorescent light mode). F = fiber, CP = cement paste, A = aggregate. **11.** Picture of V thin section taken with the optical microscope (fluorescent light mode). F = fiber, CP = cement paste, A = aggregate.

Figures 12 and 13 show pictures taken with the stereomicroscope of samples of UHPFRC-D and UHPFRC-V, respectively. As it appears, these samples are taken from specimens with a cut surface. The pictures show in both cases a compact, regular, and smooth surface. Some air bubbles entrapped in both UHPFRCs are visible, with maximum size of approximately 1 mm. Figures 14 and 15 show pictures taken with SEM with secondary electron mode of UHPFRC-D and UHPFRC-V, respectively. These pictures are taken in a magnified area of the samples previously observed with the stereomicroscope. The pictures show a fiber section and the surrounding concrete in both UHPFRCs. It is possible to clearly distinguish aggregates from the cement paste. Aggregates have a bigger maximum diameter in UHPFRC-D than in UHPFRC-V, but the nature and the microstructure seem very similar, suggesting the siliceous nature of aggregates in UHPFRC-D (which is unknown since aggregates are supplied in the commercial premix). The images highlight a very good adhesion between fibers and the cement paste.

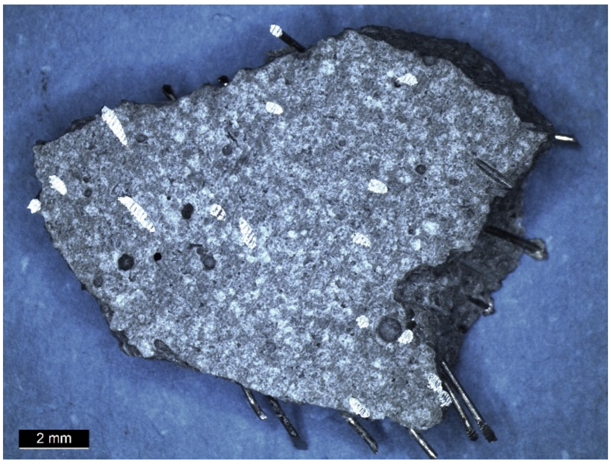

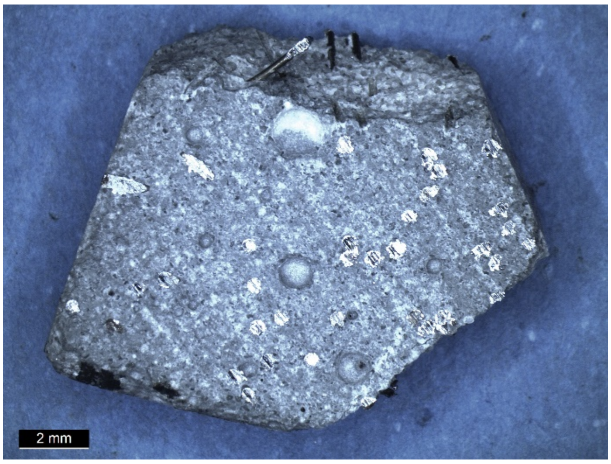

12. Picture of UHPFRC-D fragment taken with the stereomicroscope.
13. Picture of UHPFRC-V fragment taken with the stereomicroscope.

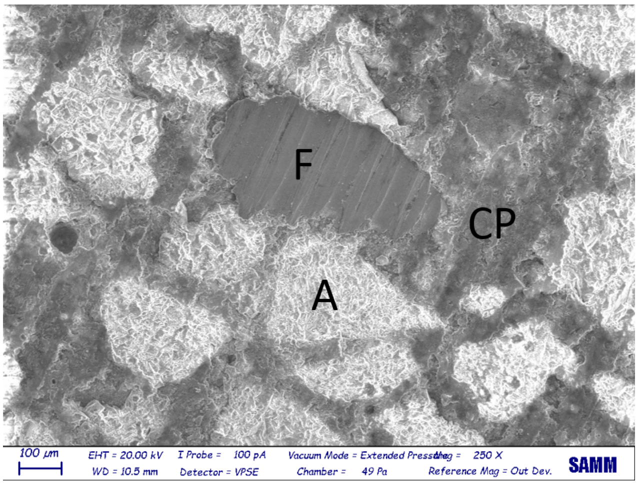

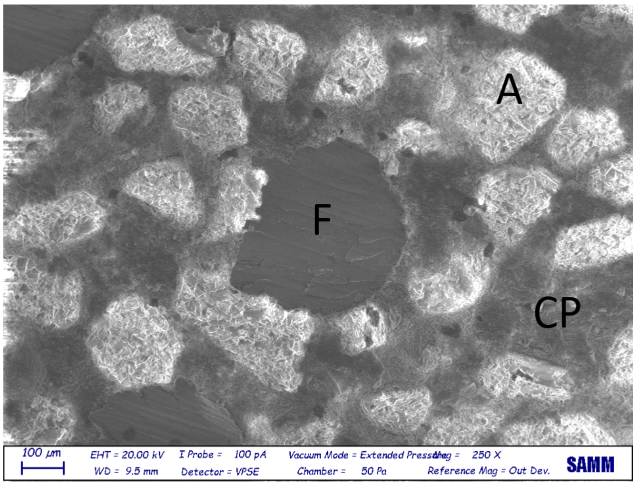

14. Picture of UHPFRC-D fragment taken with the scanning electron microscope (secondary electron mode). F = fibers, CP = cement paste, A = aggregates.
15. Picture of UHPFRC-V fragment taken with the scanning electron microscope (secondary electron mode). F = fibers, CP = cement paste, A = aggregates.

CONCLUSIONS

This note reports the results of a study aimed at characterizing the mechanical and durability properties of two commercial UHPFRCs, named D and V, with 2.5% of steel fibers in volume. For both concretes, the results show an overall excellent behavior in terms of mechanical and durability performances. Mechanical parameters (compressive strength, elastic modulus and ultra-sound velocity) are indicative of a very compact material, as well as porosity-related parameters such as water absorption, absorption rate, resistance to carbonation and chloride penetration, and also microstructural analyses. The only parameter that is similar to that of ordinary concrete is the electrical resistivity, probably due to the presence of steel fibers. As a consequence, such UHPFRCs are expected to protect embedded rebars from corrosion initiation, while their role in the corrosion propagation needs further investigation.

Regarding the role of wet curing, both materials seem to take advantage from a prolonged curing, as indicated by the increase of mechanical properties and decrease of absorption rate and water absorption with curing time. Again, the electrical resistivity shows a particular behavior since resistivity slightly decreases with curing time.

Considering the declared recipes of the two commercial products (that remain undisclosed) and the expected performances at fresh and hardened state, and comparing them with the results obtained, it can be concluded that both concretes are suitable for typical applications of UHPFRC. UHPFRC-D is characterized by lower values of porosity-related parameters, indicating a higher compactness with respect to UHPFRC-V, which, on the other hand, has a more adjustable composition since it allows the user to select certain ingredients.

BIBLIOGRAFIA | REFERENCES

[1] Russo N., Gastaldi M., Lollini F., Schiavi L., Strini A., "Studio dell'effetto delle fessure sulla durabilità del calcestruzzo armato", Structural, vol. 233, 2021.
[2] Farzad M., Shafieifar M., Azizinamini A., "Retrofitting of bridge columns using UHPC", Journal of Bridge Engineering, vol. 24, n. 12, 2019.
[3] El-Joukhadar N., Pantazopoulou S.J., "Effectiveness of UHPFRC cover in delaying bar corrosion", Construction and Building Materials, vol. 269, 2021.
[4] Cuenca E., Lo Monte F., Moro M., Schiona A., Ferrara L., "Effects of autogenous and stimulated self-healing on durability and mechanical performance of UHPFRC: Validation of tailored test method through multi-performance healing-induced recovery indices", Sustainability, n. 13(20), 2021.

[5] Corinaldesi V., Moriconi G., "Mechanical and thermal evaluation of ultra high performance fiber reinforced concretes for engineering applications", Construction and Building Materials, vol. 26, 2012.
[6] Negrini A., Roig-Flores M., Mezquida-Alcaraz E.J., Ferrara L., Serna P.," Effect of crack pattern on the self-healing capability in traditional, HPC and UHPFRC concretes measured by water and chloride permeability", Proc. 7th Int. Conf. on "Concrete Repair", MATEC Web Conf., Vol. 289, 2019, p. 1-8.
[7] Bertolini L., Elsener B., Pedeferri P., Redaelli E., Polder R.B., "Corrosion of steel in concrete: prevention, diagnosis, repair. 2nd Edition", John Wiley & Sons, 2013.
[8] Lollini F., "Cloruri e corrosione delle armature", Structural, vol. 101, 2013.
[9] Lollini F., Redaelli E., Bertolini L., "Effects of portland cement replacement with limestone on the properties of hardened concrete", Cement and Concrete Composites, vol. 46, 2014, p. 32-40.
[10] Torabian Isfahani F., Redaelli E., Lollini F., Li W., Bertolini L., "Effects of nanosilica on compressive strength and durability properties of concrete with different water to binder ratios", Advances in Materials Science and Engineering, 2016.
[11] Redaelli E., Maffezzoli B.P., Redaelli D., "Innesco e propagazione della corrosione dell'armatura in calcestruzzi fibrorinforzati ad altissime prestazioni (UHPFRC)", La Metallurgia Italiana, vol. 112, n. 4, 2020, p. 33-37.